Available online at www.sciencedirect.com

ScienceDirect

RESEARCH PAPER

Hierarchical porous activated carbon produced from spinach leaves as an electrode material for an electric double layer capacitor

Yu-jing Ou[1], Chao Peng[1,2], Jun-wei Lang[2], Dan-dan Zhu[1], Xing-bin Yan[2,*]

[1]School of Petrochemical Engineering, Lanzhou University of Technology, Lanzhou 730050, China;

[2]Laboratory of Clean Energy Chemistry and Materials, Lanzhou Institute of Chemical Physics, Chinese Academy of Science, Lanzhou 730000, China

Abstract: Hierarchical porous activated carbon (AC) was obtained by the carbonization of dried spinach leaves followed by activation with KOH. The product was characterized by nitrogen adsorption, FT-IR, FE-SEM and electrochemical tests. The AC has a dominant number of micropores, a medium number of mesopores and a few macropores with a specific surface area up to 2 616 m^2/g and a large number of oxygen-containing functional groups. The AC electrode exhibits a good double-layer capacitive behavior with a specific capacitance of 238 F/g in a 2 mol/L KOH electrolyte. A supercapacitor made of the AC has a high energy density of 10.1 Wh/Kg at a current density of 0.5 A/g and an excellent cyclic stability for 2 000 cycles over a potential range from 0 to 1.2 V.

Key Words: Spinach leaves; Activation; Activated carbon; Supercapcitor; Energy density

1   Introduction

Supercapacitors are one of the innovations in the field of electrical energy storage devices, including many excellent characteristics, such as higher specific power density and longer charge-discharge life than secondary batteries, as well as higher specific energy density than dielectric capacitors, which make them widely used in portable electronics, hybrid power sources for electrical vehicles, and uninterruptible power supply[1-3].

On the basis of fundamental mechanisms, various carbon materials, such as activated carbons[3,4], graphene[5,6], carbon nanotubes[7,8] and carbon nanofibers[9,10], generated capacitance at electrode/electrolyte interface by the formation of electric double layers. Among the carbon materials, activated carbons are the most promising electrode material for electric double-layer capacitors (EDLCs) in the supercapacitor industry due to their superior electrochemical stability, electrical conductivity. To develop supercapacitors with high performance, activated carbons are extensively activated by physical or chemical methods to increase the specific surface area of the electroactive materials. Generally, carbon electrode materials with a high specific surface area that is accessible to electrolyte ions, therefore, it is necessary to optimize pore structure, pore size and surface functionalities for charge accumulation in the electrode/electrolyte interface to form the perfect electric double-layer. In order to reduce consumption of fossil fuels,

many workers have been increasingly utilized the biomass by-products from forestry and corps residues as carbonaceous precursors for the production of activated carbons particularly in some agricultural countries with vastly available biomass residues such as fungi, argan (Argania spinosa) seed shells, sunflower seed shell, and banana fibers[11-14].

Compared with the aforementioned biomass, the spinach leaves (SLs) are abundance in China, and spinach leaf contains a great deal of stoma for photosynthesis in phytology as well as a large number of vessels and sieve-tubes in the tissue. We believed that the special structure will generate the pores after carbonization, and these pores are conducive to prepare the porous activated carbon by KOH activation at high temperatures. Herein, hierarchical porous activated carbons were synthesized from the SLs by carbonization and chemical activation with potassium hydroxide. The morphology, pore structure and specific surface area of the activated carbons were investigated by FE-SEM, DFT and BET methods. Furthermore, crystalline structure and oxygen functionality on the surface of carbon were measured using the XRD and FT-IR. Finally, the electrochemical performance of as-obtained hierarchical porous activated carbons were investigated by cyclic voltammetry (CV), galvanostatic charge/discharge (GCD) tests and electrochemical impedance spectroscopy (EIS) in KOH electrolyte.

2 Experimental

2.1 Preparation of the activated carbons from SLs

The SLs were collected from the vegetables supermarket and then air-dried at room temperature. The dried SLs were pyrolyzed at 600 $^{\circ}$C for 2 h in a horizontal tube furnace with an argon flow of 40 mL/min, to obtain carbonated products (denoted as SL-C). KOH activation of the SL-C was as follows: briefly, a given mass of SL-C was impregnated using KOH aqueous solution (the mass ratio of KOH/SL-C was 4), followed by an evaporation step at 80 $^{\circ}$C under vacuum atmosphere. The dried KOH/SL-C mixture was heated at 800 $^{\circ}$C for 1 h in the horizontal tube furnace with the same argon flow and a raising speed of 5 $^{\circ}$C / min. After being cooled down to room temperature in flowing argon flow, the product was neutralized by the 1 mol/L HCl solution until a pH value of 7 was reached. Subsequently, as-obtained activated carbons (denoted as SL-AC) was filtered, washed with ultra-pure water, and dried at 60 $^{\circ}$C in ambient for 10 h.

2.2 Structural characterization

The morphology and microstructure of the obtained products were investigated using the field emission scanning electron microscope (FE-SEM, JSM-6701F). Crystallite structures were determined by a powder X-ray diffraction (XRD, X' Pert Pro, Philips) using Cu $K\alpha$ radiation from 5° to 80°. The chemical compositions of the SL based carbon materials analyzed by Fourier transformation infrared spectroscopy (FT-IR) using a Bruker IFS66V FT-IR spectrometer. Nitrogen adsorption-desorption isotherm measurements were performed on a Micrometitics ASAP 2020 volumetric adsorption analyzer at 77 K. Prior to the adsorption experiments, all samples were adopted degassing process at 200 $^{\circ}$C for 4 h to eliminate the surface gaseous contaminants. The Brunauer–Emmett–Teller (BET) method was utilized to calculate the specific surface area of each sample and the total pore volume was estimated from the amount adsorbed at a relative pressure of $p/p_0 = 0.99$. The pore width distributions of the two carbon samples were analyzed via density functional theory (DFT) measurement.

2.3 Fabrication of activated carbon electrodes

Typically, 80% mass fraction of activated carbon material was mixed with 7.5% of acetylene black (>99.9%) and 7.5% of conducting graphite in an agate mortar until a homogeneous black powder was obtained. To this mixture, 5% of poly (tetrafluoroethylene) was added with a few drops of ethanol. After briefly allowing the solvent to evaporate, the resulting paste was pressed at 10 MPa to the nickel gauze with a nickel wire for an electric connection. The assembled electrodes were dried for 16 h at 80 $^{\circ}$C in air.

2.4 Assembly and measurements of supercapacitors

Two activated carbon electrodes fitted with a porous nonwoven cloth separator and electrolyte solution constitute the classical EDLCs. Before assembling the supercapacitor configuration, activated carbon electrodes and cloth separator were immersed in 2 mol/L KOH electrolyte to make electrolyte ions homogeneously diffuse into the porous carbon electrodes.

Electrochemical tests were carried out on an electrochemical working station (CHI660D, Shanghai, China) at room temperature. Galvanostatic charge/discharge (GCD), Cyclic voltammetry (CV) and electrochemical impedance spectroscopy (EIS) were performed to investigate the performances of the symmetrical supercapacitor.

3 Results and discussion

3.1 Microstructure characterizations of materials

Porous carbon materials with high porosity and large specific surface area were synthetized via the KOH activated the carbonaceous precursor. When the activation temperature is higher than 700 $^{\circ}$C, the plausible products of the activation reactions could include the carbon dioxide, hydrogen, carbon monoxide, potassium oxide, potassium carbonate and metallic potassium[15,16]. In this paper, the photos of fresh SLs (inset) and dried SLs were displayed in Fig. 1a. Subsequently, Fig. 1b shows some bump and rough microstructure for the SL-C material. After chemical activation, SL-AC sample exhibit a texture composed of particle on the surface of carbon materials (Fig. 1c).

The characteristics of powder XRD measurements of the two carbon samples were shown in Fig. 2a. In the XRD profiles, as-obtained SL-C sample possess two broad diffraction peaks at around $2\theta = 24.6°$ and ~43.8°, which can be attributed to the (002) and (100) crystal planes. After KOH activation for SL-C material, the peak of (002) planes has an obviously broaden and almost disappeared, and the (100) reflection plane is still present in the SL-AC sample. SL-AC carbon material has a considerable intensity in the low-angle scatter suggests the existence of a great deal of porosity[16]. Fig. 2b shows the FITR spectra of the two carbon materials for the carbonized SL and the SL-C sample was activated with the KOH agent under argon atmosphere. The carbon material of SL-C showing more intense infrared peaks compared to the sample with KOH activation. In the IR spectra, the peaks of O-H stretching vibration (3 470 cm^{-1}) and the bending vibration (1 626 cm^{-1}) were owing to surface hydroxylic groups and chemisorder water. The band at 1 066 cm^{-1} is attributed to the infrared vibration of the C-O bond. Compared with the peak of aromatic C=C double bond at 1 425 cm^{-1} is present in SL-C sample, the infrared vibration of C=C double bond for SL-AC sample shifts to a lower wavenumber due to the reaction of KOH and carbon materials. These results will be demonstrated that both carbons possess a great deal of oxygen-containing functional groups on the surface of the materials.

Nitrogen adsorption-desorption isotherms for both SLs-based carbon materials at 77 K were shown in Fig. 3a.
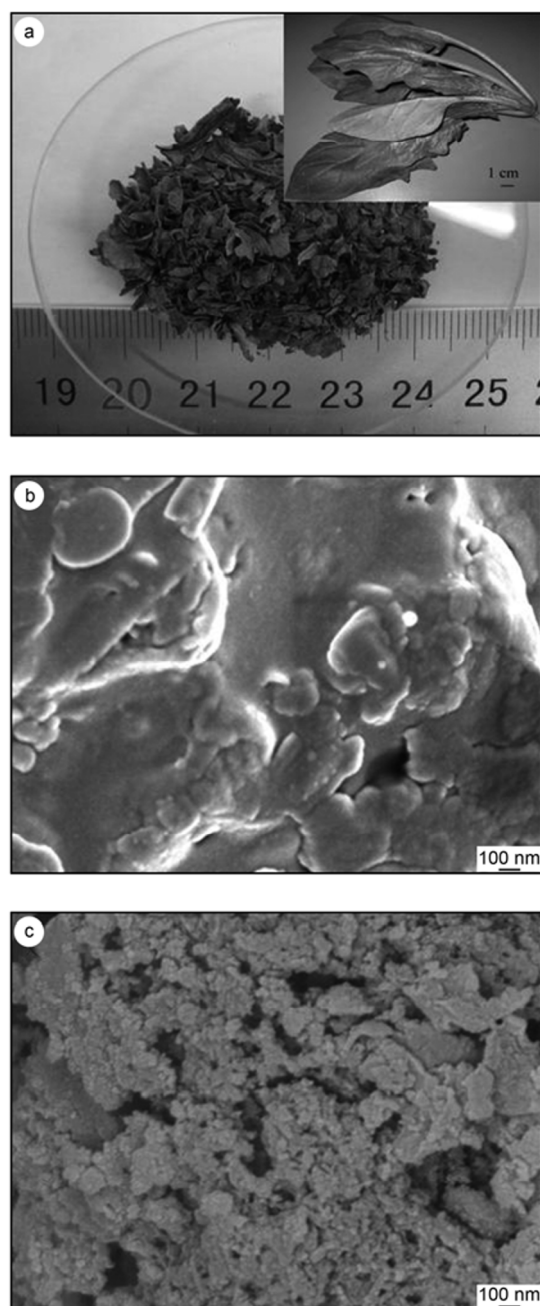
apparent enhancement in pore volume were observed from 0 for SL-C to 1.4 cm³/g for SL-AC, which indicate of activating reactions occur faster at high temperatures and more pore channels are developed[13].

3.2 Electrochemical tests for carbon electrodes in three-electrode system

The typical three-electrode cell was chosen to determine the electrochemical performance of the carbon materials coated nickel foam in KOH electrolyte. As shown in Fig. 4, the CV and GCD curves were used to characterize the capacitive behavior of as-prepared SL-C and SL-AC electrodes in 2 mol/L KOH electrolyte. The CV curves of the SL-AC electrode in our experiment exhibit relatively rectangular in Fig. 4a, indicating that most of the ion charges were stored by the electric double-layer mechanism for SL-AC electrode[20]. At the same time, it can be seen that the area of SL-AC electrode is higher than that of the SL-C electrode, suggesting SL-AC electrode possess the high specific capacitance. Moreover, the results of galvanostatic charge-discharge process for the two carbon materials at current density of 1 A/g were shown in Fig. 4b, and the specific capacitances are 232 and 19 F/g corresponding to the SL-AC and SL-C electrodes, respectively. It can be observed that the specific capacitance of SL-AC obviously higher than that of SL-C with KOH electrolyte at the same current density of 1 A/g, which can be attribute to the SL-AC possess the ideal hierarchical porous structure including the domination of

Fig. 1 (a) Digital image of dried SLs (inset is the fresh SLs); the FESEM images of (b) SL-C

SL-AC sample represent with characteristic of the type IV due to the sharp increase at low relative pressure is attributed to the existence of micropores, and desorption hysteresis at medium relative pressure suggests the presence of developed mesoporosity[17-19]. Furthermore, observation from the pore size distribution of Fig. 3b, the hierarchical porous material of SL-AC is consisted of the most of micropores, mesopores and a part of macroporosity. However, in contrast, Fig. 3b exhibits that the SL-C material is composed of mesopores and macroporosity. As shown in Fig. 3, it can be seen that the shapes for SL-C and SL-AC are very distinctive, and the specific surface area of SL-AC (2 616 m²/g) is higher than that of SL-C (2 m²/g). Meanwhile, an
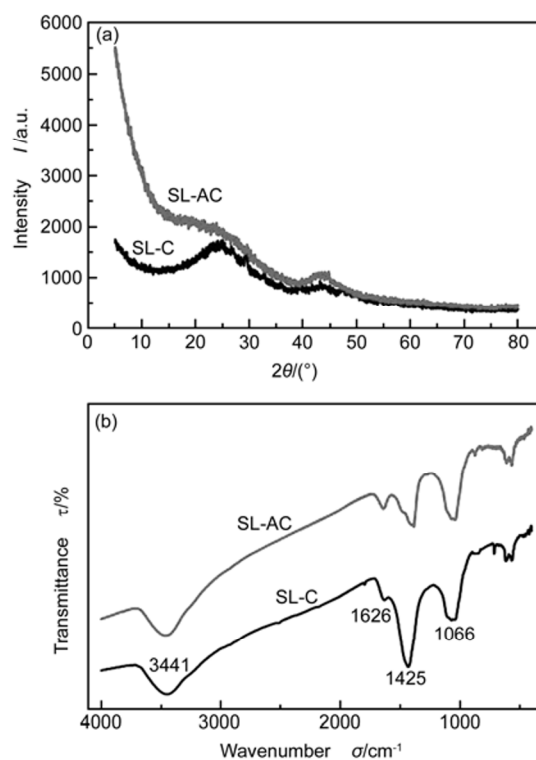

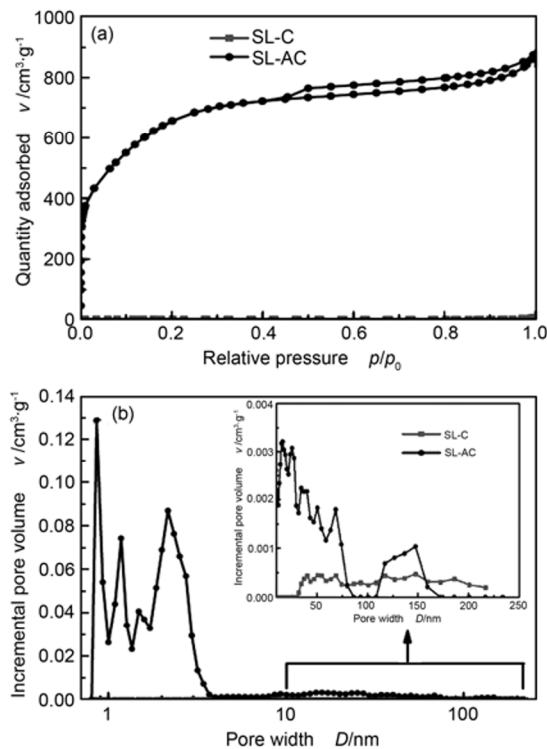Fig. 2 The SL-C and SL-AC carbon samples: (a)XRD patterns and (b)FI-TR spectra.

Fig. 3 (a) Nitrogen adsorption-desorption isotherms and (b) pore size distributions for the SL-C and SL-AC carbon materials.
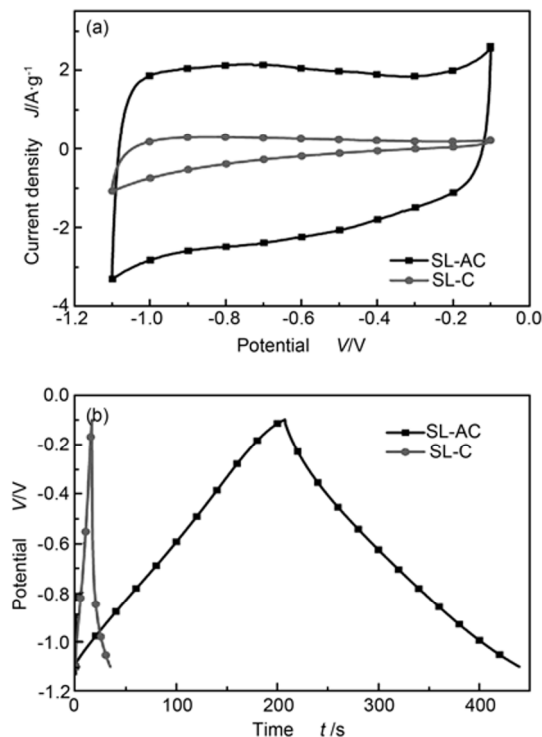

Fig. 4 Electrochemical measurements of SL-C and SL-AC: (a) at the sweep rate of 10 mV/s and (b) at the current density of 1 A/g.

the micropores, mesopores and a part of macroporosity.

However, the few micropore leaded to the low specific capacitance for the SL-C electrode. The optimization porous structures are conducive to generate the compact electric double layer and excellent transmission channel of the electrolyte ions[21].

3.3 Electrochemical tests for activated carbon electrodes in two-electrode system

In order to further investigate the electrochemical capacitive performances for the activated carbon electrodes, the symmetry EDLCs was fabricated with those of carbon electrodes of SL-AC and KOH aqueous solution as electrolyte.

Fig. 5a shows two-electrode CV curves obtained from SL-AC based EDLCs with KOH electrolyte at sweep rates of 10, 20, 50 and 100 mV/s, whose potential window were chosen in the range of 0 to 1.2 V. In the electrochemical capacitors, it is clear that ideal rectangular shapes were maintained even at a high scan rate of 100 mV/s, which indicates the excellent reversibility and fast ionic transport of the symmetric EDLCs with SL-AC electrodes.

The ability to charge and discharge at high current is a crucial characteristic for supercapacitors because of the high power demand from portable electronic power source and electric vehicles. The representative GCD curves of the symmetry EDLCs at constant current density range from 0.5 to 10 A/g were shown in the Fig. 5b. It can be seen that SL-AC based EDLCs possess longer charge time than the discharge time at the current density of 0.5 A/g, resulting from partial pseudo-capacitance generated in positive and negative electrodes owing to the oxygen-containing on the surface of carbon materials. GCD curves at the current density range from 1 to 10 A/g exhibit good triangle-shapes and excellent coulomb efficiency, and the specific capacitance of 41 and 33 F/g at current density of 1 and 10 A/g, respectively. The capacitance retention is as high as 80%, indicating the rapid charge and discharge capability for the symmetric EDLCs with SL-AC electrodes. The capacitance of single electrode in symmetric EDLC was approximately four times that of the two-electrode symmetric cell[22]. Therefore, the specific capacitance for each electrode of the symmetric cell is 164 F/g at the current density of 1 A/g in 2 mol/L KOH electrolyte.

EIS was utilized to investigate the performances of supercapacitor in the frequency range of $10^5 \sim 10^{-2}$ Hz, such as frequency response and equivalent series resistance (ERS)[23,24]. As shown in Fig. 5c, symmetric EDLCs present very ideal impedance characteristics, because the semicircle of small radius is obtained at high frequency range (inset) due to low electronic resistance between the activated carbon material, and the near vertical Warburg diffusion segment at low frequency range is attributed to the ion diffusion in the structure of the electrodes possess an ideal supercapacitor behaves. The value of ERS for SL-AC is 0.36 Ω from the X-intercept of the Nyquist plot in Fig. 5c for SL-AC based EDLCs. The low ERS and small Warburg diffusion resistance
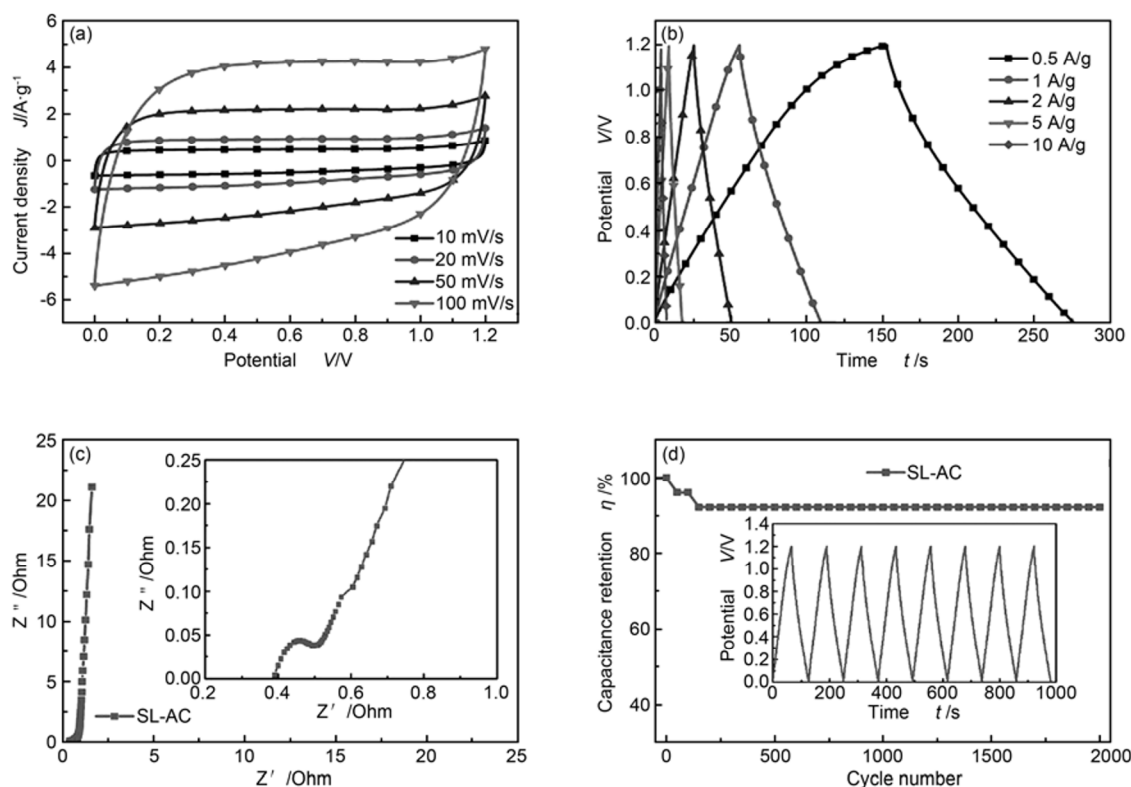
Fig. 5 Electrochemical performances for symmetric EDLCs with a two-electrode: (a) CV profiles for SL-AC at different of scan ratio; (b) GCD curves at current density range from 0.5 to 10 A/g; (c) Nyquist plot and inset is the enlarged plot of the high-frequency region; (d) Relationship between capacitance retention and cycle number of supercapacitor at the current density of 2 A/g, inset is the final eighty cycles.
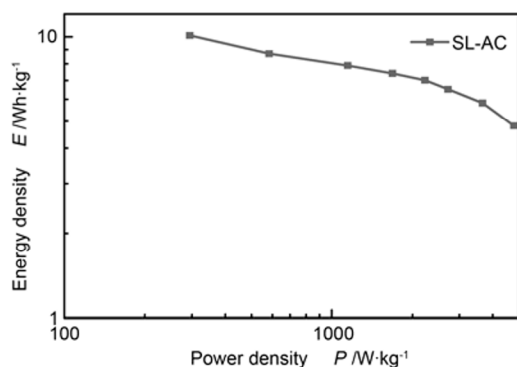

Fig. 6 The Ragone plot for symmetric EDLCs with the SL-AC electrodes.

resulted from the hierarchical porous structure of SL-AC, which was prepared via carbonization and KOH activation process of SLs.

Fig. 5d shows the stabilities of the symmetry EDLCs during a charge-discharge process in the potential range from 0 to 1.2 V with a constant current density of 2 A/g. There is a slight loss of capacitance in the first 150 cycles owing to the irreversible reaction between the electrolyte and electrodes, and then remain almost constant[25]. The starting capacitance decreased by 7.8% for SL-AC EDLCs after 2 000 charge-discharge process. For the final eighty cycles, the charge-discharge curve exhibits the good linearity and the time of charge and discharge are similar equality.

The energy density and power density are calculated by the GCD measurements at different current density[26]. Finally, the Ragone plot for symmetric EDLCs with the SL-AC electrodes in 1.2 V KOH electrolytes is shown in Fig. 6, which exhibits the energy density deceases with the increase of power density. The energy density of the symmetric EDLCs reach to 10.1 Wh/kg at the current density of 0.5 A/g and the power density is 4 800 W/kg, which is superior to the performance of the reported carbon materials due to the energy density is proportional to the square of the voltage window[27, 28].

4   Conclusions

Hierarchical porous carbon material of SL-AC was successfully prepared by pyrolysis of the dried spinach leaves (SL) and following activation with KOH. As-obtained hierarchical porous carbon materials exhibit a texture consist of like-particle, a large number of oxygen-containing functional groups on the surface of material and the specific surface area up to 2 616 m^2/g. Electrochemical results suggest SL-AC activated carbons have good capacitive behaviour about rectangular and triangular characteristics corresponding to the cyclic voltammetry and galvanostatic charge-discharge curves. Assembled the symmetry EDLCs possess low ERS

and excellent cyclic stability after 2 000 cycles in KOH electrolyte, as well as high energy density of 10.1 Wh/kg in the voltage window of 1.2 V.

References

[1] Sofiane B, Kara E, Gleb Y. Atomic layer deposition of vanadium oxide on carbon nanotubes for high-power supercapacitor electrodes [J]. Energy Enviro Sci, 2012, 5: 6872-6879.

[2] Zhang D C, Zhang X, Chen Y, et al. An environment-friendly route to synthesize reduced graphene oxide as asupercapacitor electrode material [J]. Electrochim Acta, 2012, 69: 364-370.

[3] Sun X Z, Zhang X, Zhang D C, et al. Activated carbon-based supercapacitors using Li_2SO_4 aqueous electrolyte [J]. Acta Phys-Chim Sin, 2012, 28: 367-372.

[4] Anouti M, Couadou E, Timperman L, et al. Protic ionic liquid as electrolyte for high-densities electrochemical double layer capacitors with activated carbon electrode material [J]. Electrochim Acta, 2012, 64: 110-117.

[5] Zhang S L, Li Y M, Pan N. Graphene based supercapacitor fabricated by vacuum filtration deposition [J]. J Power Sources, 2012, 206: 476-482.

[6] Yan J, Liu J P, Fan Z J, et al. High-performance supercapacitor electrodes based on highly corrugated graphene sheets [J]. Carbon, 2012, 50: 2179- 2188.

[7] Hu Y, Zhao Y, Li Y, et al. Defective super-long carbon nanotubes and polypyrrole composite for high-performance supercapacitor electrodes [J]. Electrochim Acta, 2012, 66: 279-286.

[8] Alzubaidi A, Inouet T, Matsushita T, et al. Cyclic voltammogram profile of single-walled carbon nanotube electric double-layer capacitor electrode reveals dumbbell shape [J]. J Phys Chem C, 2012, 116: 7681-7686.

[9] Liu S, Song Y, Ma C, et al. The electrochemical performance of porous carbon nanofibers produced by electrospinning [J]. New carbon materials, 2012, 27: 129-134.

[10] Kim B H, Yang K S, Kim Y A, et al. Solvent-induced porosity control of carbon nanofiber webs for supercapacitor [J]. J Power Sources, 2011, 196: 10496-10501.

[11] Zhu H, Wang X L, Yang F, et al. Promising carbon for supercapacitors derived from fungi [J]. Adv Mater, 2011, 23: 2745-2748.

[12] Elmouwahidi A, Zapata B Z, Carrasco M F, et al. Activated carbons from KOH-activation of argan (Argania spinosa) seed shells as supercapacitor electrodes [J]. Bioresour Technol, 2012, 111: 185-190.

[13] Li X, Xing W, Zhuo S P, et al. Preparation of capacitor's electrode from sunflower seed shell [J]. Bioresour Technol, 2011, 102: 1118-1123.

[14] Subramanian V, Luo C, Stephan A M, et al. Supercapacitors from activated carbon derived from banana fibers [J]. J Phys Chem C, 2007, 111: 7527-7531.

[15] Yuan M J, Kim Y, Jia C Q. Feasibility of recycling KOH in chemical activation of Oil-sand petroleum coke [J]. Can J Chem Eng, 2012, 90: 1472-1478.

[16] Zhu Y W, Murali S, Stoller M D, et al. Carbon-based supercapacitors produce by activation of grapheme [J]. Science, 2011, 332: 1537-1541.

[17] Lv Y K, Gan L H, Liu M X, et al. A self-template synthesis of hierarchical porous carbon foams based on banana peel for supercapacitor electrodes [J]. J Power Sources, 2012, 209: 152-157.

[18] Lu H L, Dai W J, Zheng M B, et al. Electrochemical capacitive behaviors of ordered mesoporous carbons with controllable pore sizes [J]. J Power Sources, 2012, 209: 243-250.

[19] Chen W X, Zhang H, Huang Y Q, et al. A fish scale based hierarchical lamellar porous carbon material obtained using a natural template for high performance electrochemical capacitors [J]. J Mater Chem, 2010, 20: 4773-4775.

[20] Choi D, Kumta P N. Synthesis, structure, and electrochemical characterization of nanocrystalline tantalum and tungsten nitrides [J]. J Am Ceram Soc, 2007, 90:3113-3120.

[21] Zhang G Q, Zhang S T. Characterization and electrochemical applications of a carbon with high density of surface functional groups produced from beer yeast [J]. J Solid State Electr, 2009, 13: 887-893.

[22] Stoller M D, Ruoff R S. Best practice methods for determining an electrode material's performance for ultracapacitors [J]. Energy Enviro Sci, 2010, 3: 1294- 1301.

[23] Rose M, Korenblit Y, Kockrick E, et al. Hierarchical micro- and mesoporous carbide-derived carbon as a high-performance electrode material in supercapacitors [J]. Small, 2011, 7: 1108-1117.

[24] Wei L, Sevilla M, Fueres A B, et al. Hydrothermal carbonization of abundant renewable natural organic chemicals for high-performance supercapacitor electrodes [J]. Adv Energy Mater, 2011, 1: 356-361.

[25] Wang Y G, Xia Y Y. Hybrid aqueous energy storage cells using activated carbon and lithium-intercalated compounds [J]. J Electrochem Soc, 2006, 153: 450-454.

[26] Lang J W, Yan X B, Liu W W, et al. Influence of nitric acid modification of ordered mesoporous carbon materials on their capacitive performance in different aqueous electrolytes [J]. J Power Sources, 2012, 204: 220- 229.

[27] Yu H J, Wu J H, Fan L Q, et al. Improvement of the performance for quasi-solid-state supercapacitor by using PVA-KOH-KI polymer gel electrolyte [J]. Electrochim Acta, 2011, 56: 6881-6886.

[28] Jagannathan S, Chae H G, Jain R, et al. Structure and electrochemical properties of activated polyacrylonitrile based carbon fibers containing carbon nanotubes [J]. J Power Sources, 2008, 185: 676-684.